

Sound Reflections from Concave Spherical Surfaces. Part II: Geometrical Acoustics and Engineering Approach

Martijn Vercammen

Peutz bv, Lindenlaan 41, PO Box 66, 6585 ZH, Mook, The Netherlands. m.vercammen@mook.peutz.nl

Summary

Focussing arising from concave surfaces has long been a well-known problem in room acoustics. The focussing can cause high sound pressure levels, colouration or an echo. Part I of this paper [1] provides a mathematical approximation based on wave extrapolation of the sound field in and around the focal point due to reflections by a spherical surface. This second part of the paper provides some practical methods for calculating the sound field. A geometrical approach is presented, the limitations of image source methods are described and an engineering method is presented. Computer models based on image source methods are not capable of describing the pressure in or out of the focal. The sound field outside the focal area can be calculated within reasonable accuracy with a geometrical approach. The results show that for a small wavelength the focussing effect is fairly strong. Generally the possible reduction of the focussing effect by absorbers or diffusers is not enough to eliminate the focussing effect by spherical surfaces.

PACS no. 43.55.Br, 43.55.Ka

1. Introduction

The focussing effect of curved surfaces in room acoustics is well-known, although quantification has long been a puzzle. The concentration of reflections can be the cause of most serious acoustic defects such as echoes, flutter echoes, unbalanced amplification and incorrect source localisation. Many textbooks describe the phenomenon, and the best way to illustrate the concentration is with geometrical acoustics, representing the propagating sound waves by rays. Figure 1 shows a 17th century example of such an illustration.

Many authors of standard books on acoustics point out the danger of concave surfaces (e.g. [2, 3, 4, 5], this phenomenon is described in many more textbooks) but do not give an estimate or calculation method for the sound pressure in the focus.

Nowadays acousticians are certainly well aware of the potential risk of sound concentration. In small rooms and small halls there will be one or more spots where the sound level is much higher and may sound different due to different amplification at different frequencies (see paragraph 3.2).

In larger halls the time difference between direct sound and concentrated reflection may be large enough to detect audible echoes. The question as to when the reflection will

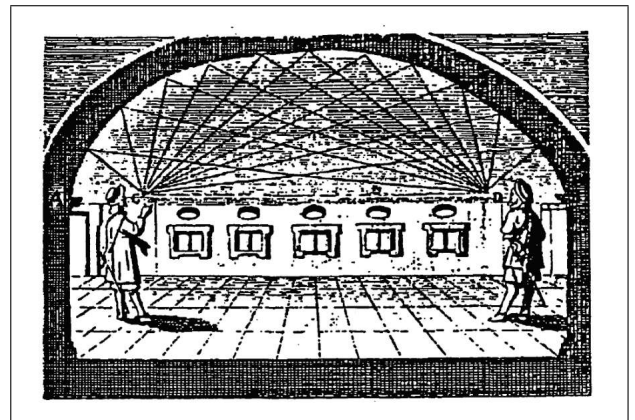


Figure 1. Illustration of the focussing effect by an ellipse [6].

be heard as colouration or as a distinct echo is an interesting topic, but is outside the scope of this paper. Generally it is considered that the reflection will not be heard as a separate echo should it arrive within 50 ms after the direct sound.

However, not in all cases; concentration due to reflection against a concave surface needs to be considered as negative.

In the 17th century, vaults were recommended for enhancing speech intelligibility (e.g. ‘echometria’, the art of creating echoes, in [7]). Figure 1 illustrates the speech enhancement at the listener’s position [6].

With designers unaware of the danger of echoes and unbalanced amplification, ellipse floor plans were recom-

Received 18 March 2009,
accepted 20 October 2009.

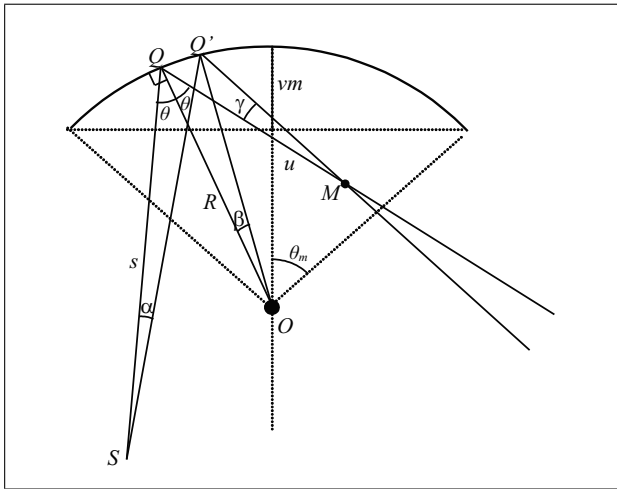


Figure 2. Geometry showing the concave surface with source position S and position of the focal point M .

mended for theatres at the end of 18th century, e.g. by [8], to enhance the low levels at the back rows. The enhancement of reflected sound by concave surfaces can be acceptable or even advantageous in small halls (an excellent example of this is the London Wigmore Hall for chamber music [9]); in larger halls it will lead to strong late reflections that can be heard as an echo. These echoes are very persistent and although it can be done, it often turns out to be a difficult job to get rid of them (e.g. in the Royal Albert Hall [2] and [10], the Tonhalle Düsseldorf [11] and Haus des Lehrers, Berlin [12]). In architecture a development can be seen, supported by developments in computer aided design, towards the use of expressive curved shapes, both in exteriors and interiors. There is clearly a need for practical room acoustical prediction methods to describe the sound field in these types of spaces without having to use a scale model. The purpose of this paper is to present engineering tools to predict the sound field in these spaces. A geometrical approach is described in section 2. With this method the increasing sound pressure resulting from the concentration of energy over a smaller cross-section is calculated. At the focal point the area of this cross-section approaches zero and the calculated pressure will be infinite, while in reality there will be a spread of energy over an area, related to the wavelength.

The sound pressure at the focus can only be calculated correctly by incorporating the wave character into the calculation method. In Part I of this paper [1] exact values and approximations of the sound pressure at the focus and in the area around the focus for reflections from concave spherical surfaces are given, based on the wave field approach. The results of this work are used in section 3 where an engineering method is given to estimate the sound field due to reflections from concave surfaces.

This paper will concentrate on reflections from a spherically-curved surface, e.g. a hemisphere or a sphere segment. For comparison, results from literature of reflections from cylindrically-shaped surfaces will also be shown.

In section 4 the results of different computer applications of geometrical methods are compared to the wave theoretical results.

Reducing the reflection strength will be discussed in section 5, also showing why it is so difficult to reduce the echoes due to reflections from concave surfaces. Conclusions are drawn in section 6.

2. Geometrical acoustics

2.1. Focussing

Figure 2 shows the geometrical situation with a hard, fully reflecting, concave surface characterised by the radius R , a source position S at distance s and a resulting focal point M at distance u .

The geometry shows that

$$QQ' = \frac{s \sin \alpha}{\cos \theta} = \frac{u \sin \gamma}{\cos \theta} = R \sin \beta.$$

For small angles of α , β and γ

$$s\alpha = u\gamma = R\beta \cos \theta.$$

This will give $u = s\alpha/\gamma$ and $\beta = s\alpha/(R \cos \theta)$ and from the summation of the angles of the three triangles: $\gamma = 2\beta - \alpha$.

This will result in

$$\frac{1}{u} + \frac{1}{s} = \frac{1}{f \cos \theta} \quad (1)$$

with $R = 2f$.

This is known (usually for normal incidence with $\cos \theta = 1$) as the thin lens formula.

The reflected sound field can also be considered as a spherical sound field expanding from M . For geometric acoustic modelling the focal point position M can be used as a mirror source in analogy with Image Source Method (ISM). The position of this point can be the basis of the calculation of the reflected sound field.

Contrary to mirror sources caused by flat mirrors, the mirror source for concave reflecting surfaces is in the space, unless the source is between $R/2$ and the reflector. In the latter case the sound field will be diverging and u will be negative. This paper considers only the concentrating sound fields with $s > f$.

The pressure of the sound field incident at Q on the reflector can be described by

$$p(s) = \hat{p} \frac{e^{-jks}}{s},$$

where k is the wavenumber and \hat{p} the amplitude (in N/m) corresponding to the value of the pressure amplitude at 1 m from the source.

The geometrically-reflected sound field can be described using the position of the focal point as a reference.

The pressure will depend on the distance r_M to the focal point, presuming r_M is in the illuminated area (see Figure 3),

$$p(r_M) = X \frac{e^{-jk(s+u+r_M)}}{r_M}.$$

The amplitude X can be determined by setting the pressure from the source and the (mirror) source at the focal point equal at the surface of the concave reflector,

$$\hat{p} \frac{e^{-jks}}{s} = X \frac{e^{-jku}}{u}.$$

Assuming equal phase for the incident and reflected sound for each position at the mirror, this means that the amplitude of the mirror source will be

$$X = \hat{p} \frac{u}{s}.$$

The reflected sound field can now be described by

$$\begin{aligned} p(r_M) &= \hat{p} \frac{m e^{-jk(s+u+r_M)}}{s |r_M|} \\ &= \hat{p} \frac{R \cos \theta}{2s - R \cos \theta} \frac{e^{-jk(s+d)}}{|d-u|}, \end{aligned} \quad (2)$$

where $d = u + r_M$. At $d = u$ (the mirror source M) the calculated sound pressure according to (2) will be infinite. In reality it will be finite and the pressure will depend on the wavelength and the size of the mirror. Outside this focal point the amplitude does not depend on the size of the mirror; the reception point is either visible or not. The visibility check is basically similar to ordinary mirror sources. The mirror source is visible (or “a reflection has to be calculated”) when a line from the receiver point through the mirror source hits the concave surface. The area where this is the case, the illuminated area, is shown in Figure 3. The difference from normal mirror sources is that for flat surfaces the surface is between the reception point and the mirror source. With concave surfaces the mirror source is between the reception point and the reflecting surface.

It can be concluded that it is geometrically possible to use the concept of a mirror source with concave spherical surfaces, and the mirror image is then located inside the space. The amplitude and time delay from the mirror source and the visibility check have to be adapted. For other surface shapes, such as cylindrical shapes, this is not possible, since there is not a single focal point.

2.2. Amplification by curved surfaces

At distance d from a flat surface the amplitude of the reflection will be

$$|p(d)| = \frac{\hat{p}}{s+d}.$$

Using (2), the amplification of the pressure from the spherically-concave surface, relative to the flat surface, will be

$$q = (s+d) \frac{u}{s} \frac{1}{d-u} \Rightarrow \frac{1}{q} = \frac{1}{\frac{1}{d} + \frac{1}{s}} R \cos \theta - 1. \quad (3)$$

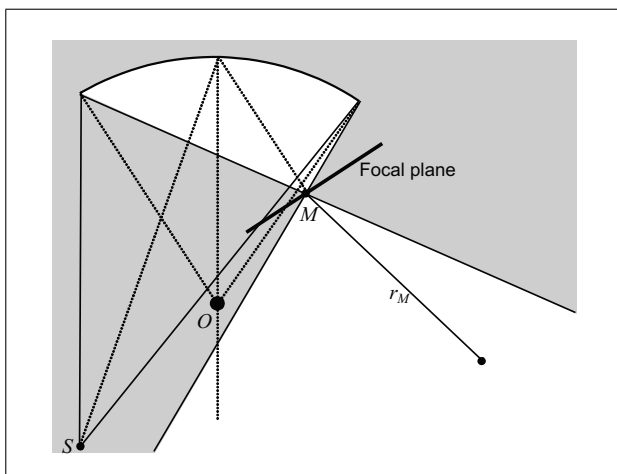


Figure 3. Geometry showing the illuminated reflection area in white and the receiver at distance r_M . The area outside the illuminated area is a shadow zone for the reflection.

The sound pressure level increase will be

$$\Delta L = -20 \log \left(\frac{1}{\frac{1}{d} + \frac{1}{s}} \frac{2}{R \cos \theta} - 1 \right). \quad (4)$$

This corresponds to the expressions given by [4] and [13]. This will be not defined for

$$\frac{1}{\frac{1}{d} + \frac{1}{s}} = \frac{1}{2} R \cos \theta,$$

e.g. for $d = s = R$, $\theta = 0$.

This is the basic limitation of the geometric model. To approximate the pressure in the focal area a wave theoretical approach is needed, as presented in the next section.

3. Engineering method

In the first part of this paper [1] a wave theoretical approach is presented for calculating the sound field from a spherical reflector. It is found that, apart from the interference pattern, at sufficient distance from the focal point the sound field can be described by geometrical methods. For room acoustical purposes, the wave theoretical approach is only necessary for the area around the focal point. In this section the main results of the pressure at the focus, in the focal plane and along the focal axis are discussed.

3.1. Pressure at the focal point

The situation will be considered of a hard spherical reflector with an opening angle θ_m (see Figure 2). The depth of the spherical reflector vm (from vertex to mouth, see Figure 2) is more than a wavelength λ ($vm = R(1 - \cos \theta_m) > \lambda$). This will result in a focussing effect.

For smaller depth vm , the focussing will be less and for $vm < \lambda/4$ the focussing will not occur (only diffraction, see [1]).

The pressure in a receiver position can be calculated from the pressure on the surface of the reflector. At every

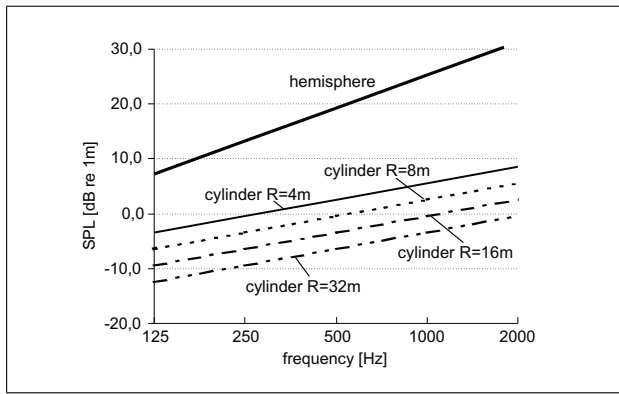


Figure 4. The Sound pressure level (relative to the SPL at 1 m from the source) at the focal point or focal line for a hemisphere (9) and a half cylinder with radius $R = 4, 8, 16$ and 32 m (10). The SPL of the hemisphere is independent of the radius.

position on the reflector a secondary source will radiate and the pressure in the receiver position results from integration of the contributions of all these secondary sources. If the source S is located in the centre of the sphere O , the pressure at the focal point M can easily be calculated ([1]):

$$|p_M| = k\hat{p}(1 - \cos \theta_m). \quad (5)$$

The sound pressure level (SPL) at the focal point, relative to the SPL at 1 m from the source, is

$$\Delta L = 10 \log k^2(1 - \cos \theta_m)^2. \quad (6)$$

For a hemisphere ($\theta_m = \pi/2$) this will be

$$|p_M| = k\hat{p}, \quad (7)$$

$$p_{M\text{rms}}^2 = \hat{p}^2 k^2 / 2, \quad (8)$$

$$\Delta L = 10 \log k^2. \quad (9)$$

It is noted that the increase in sound pressure level only depends on the opening angle and frequency and not on the radius of the (hemi)sphere. All energy radiated in the (hemi)sphere returns to the centre, independently from the radius.

Should the source position not correspond to the centre of the sphere, the position of the focal point can be found by construction of the specular line and calculating the distance u according to the thin lens formula (1). For a first approximation of the level increase (6) may be used; however this sound pressure level increase is only accurate for the situation where the source and the receiver are close to the centre. In the case of a larger distance from the centre, the maximum SPL at the focal point will be lower, see [1].

For comparison the maximum pressure increase (in dB relative to the SPL at 1 m) at the focal line of a half circular cylinder (closest to the source) can be obtained from [14] and [15]:

$$\Delta L = 10 \log \left(\frac{\pi k}{4R} \right). \quad (10)$$

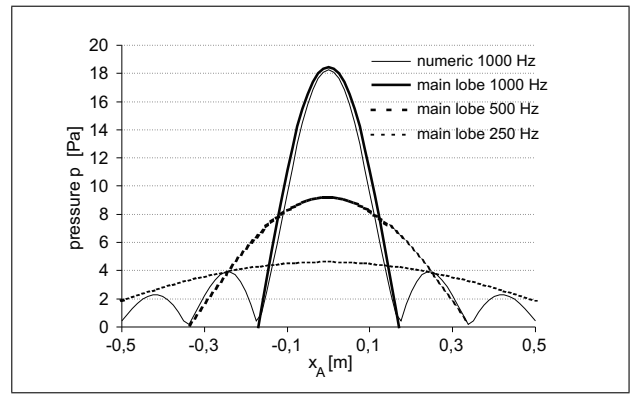


Figure 5. Calculation example of the pressure in the focal plane of a hemisphere (with $\hat{p} = 1$ N/m). Numerical solution [1] and the main lobe with (11) for 1000 Hz. Also showing the main lobe for 500 and 250 Hz.

It is noted that for a cylinder the ΔL is dependent on the radius of the cylinder, since there is a concentration in one direction and convergence in the other (along the axis of the cylinder).

Figure 4 shows the SPL at the focal point for some different conditions.

It shows that the focussing effect of a spherical reflector is much stronger than the focussing effect of a cylinder.

When comparing the level of the reflection relative to the direct sound at the receiver position, the level decrease of the direct sound has to be added ($10 \log(s_0^2)$, with s_0 : distance source-receiver). At e.g. 8 m distance the SPL of the reflection at the focal point will be approx. $(19+18=)$ 37 dB above direct sound at 500 Hz. Both this example and Figure 4 show that the amplification at the focal point can be quite dramatic, especially for spherically-curved structures.

3.2. Pressure in the focal plane

The focal plane is the plane through the focal point M and the normal to the main axis of the sphere segment. The pressure in this focal plane will be high at the centre (focal point), rapidly decreasing outside the centre, with some remaining side lobes due to interference (see [1]). Assuming we are only interested in the high sound pressure levels around the focal area it is sufficient to define the main lobe. This main lobe can be expressed by

$$|p(x_A)| \approx \hat{p}k(1 - \cos \theta_m) \cos(\frac{1}{2}x_A k \sin \theta_m), \quad (11)$$

where x_A is the distance to M in the focal plane. A calculation example is given in Figure 5. The width of the focussing area (-3 dB points) is $x_A \approx \pm \lambda / (4 \sin \theta_m)$. At the focal (x, y) plane ($z_A = 0$) of a hemisphere ($\theta_m = \pi/2$) the focussing area will be a circle with a diameter of half a wavelength,

$$S_M \approx \pi \left(\frac{\lambda}{4 \sin \theta_m} \right)^2 = \frac{\pi}{16} \lambda^2.$$

The sound power P_S of a sound source can be written (20) $P_S = 2\pi\hat{p}^2 / \rho c$.

The power from a sound source in the centre, incident on a hemisphere, will be half this value: $P_S = \pi \hat{p}^2 / \rho c$. This sound power will be reflected towards the focal point.

When distributing this sound power over the focussing area S_M the rms pressure will be $p_{\text{rms}}^2 = \rho c P_S / S_M \approx 0.4 \hat{p}^2 k^2$; this is close to the theoretical peak value (8).

So for a hemisphere, the energy is distributed over a circular area with a width of approximately half a wavelength. Outside this circular area the receiver is either in the shadow zone (Figure 3) and the SPL will decrease rapidly, or it will be in the illuminated area (only for $\theta_m \geq \pi/2$) and the average SPL (without interference) can be estimated with geometrical methods.

The practical meaning of this distribution function is that the area where the focussing effect can be noticed is much larger for the lower frequencies than for the higher ones (see also Figure 5). For example a receiver positioned at 0.3 m from the geometrical focal point is outside the focal area at 1000 Hz, however for the 250 Hz signal this point is still within the focal area. So the amplification will be strongly frequency-dependent. Since the area where the low frequency amplification occurs is much larger, focussing problems are mostly perceived as rather low or middle frequency problems.

3.3. Pressure along the focal axis

When looking along the specular axis, with d : the distance from the reflecting surface, the amplitude of the pressure can be described by [1]

$$|p(d)| = \left| \frac{2\hat{p}}{sd \left(\frac{1}{d} + \frac{1}{s} - \frac{2}{R} \cos \theta \right)} \cdot \sin \left(\frac{1}{2} k R^2 (1 - \cos \theta_m) \left(\frac{1}{d} + \frac{1}{s} - \frac{2}{R} \cos \theta \right) \right) \right| \quad (12)$$

After the first zero the pressure can be approximated by the geometrical field, by (2). This first zero (with the $\sin()$ in (12) set to π) will occur at

$$\frac{1}{d} = \pm \frac{\lambda}{R^2(1 - \cos \theta_m)} - \frac{1}{s} + \frac{2}{R} \cos \theta. \quad (13)$$

Figure 6 illustrates these approximations in a calculation example. It is shown that the approximation agrees quite well with the numeric solution. The geometrical solution is to be considered as an average of the oscillating reflected sound field and can be applied outside the points defined by (13).

4. The use of room acoustical computer models

Wave phenomena such as the amplification at the focal point can be simulated when solving the wave equation with the use of finite element programs in which the size of the elements is smaller than the wavelength (e.g. BEM, FEM, FDTD). The use of these programs however is not yet common, mainly due to extremely long calculation

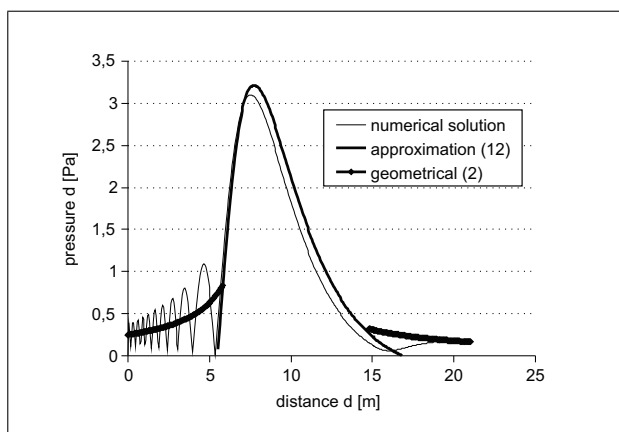


Figure 6. The sound pressure along the axis in a calculation example: $R = 5.4$ m, $f = 1000$ Hz, $\theta_m = 0.2\pi$, $\theta = 0$, $s = 4$ m ($u = 8.3$ m); numerical solution (see [1]), approximation with (12) between the zeros given by (13) and the geometrical field by (2).

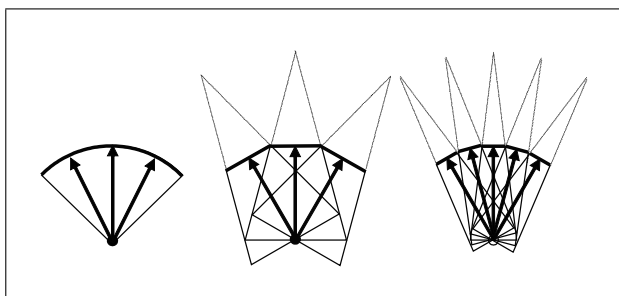


Figure 7. Segmenting a curved surface by plane surfaces.

times and difficulties in defining boundary conditions (e.g. [16]).

In the practice of room acoustics, computer modelling is based on geometrical acoustics, using the Image Sources Method (ISM), Ray Tracing (RT) or Beam Tracing (BT).

In these models curved (sphere) elements are not to be modelled as curved elements but are replaced by small plane surfaces, segmenting the curved element (see Figure 7). Depending on the shape of the curved segment, they are modelled as rectangle, trapezium or triangle planes. This segmenting will influence the calculated pressure at the focal point.

In this section the use of geometrical computer modelling will be discussed, mainly the influence of segmenting the curved surface. This influence will also depend on the method used.

4.1. Image source method

Assuming the area of the planes will be b^2 (the planes have a characteristic dimension b), the number of mirror images for a hemisphere will be $N = 2\pi R^2 / b^2$. The Image Source Method (ISM) is based on the addition of energy from the mirror sources. In this case the pressure at distance r from a sound source can be written by $p(r)_{\text{rms}}^2 = 1/2 \hat{p}^2 / r^2$. With the source in the centre of a hemisphere, the pressure in the centre due to the mirror sources

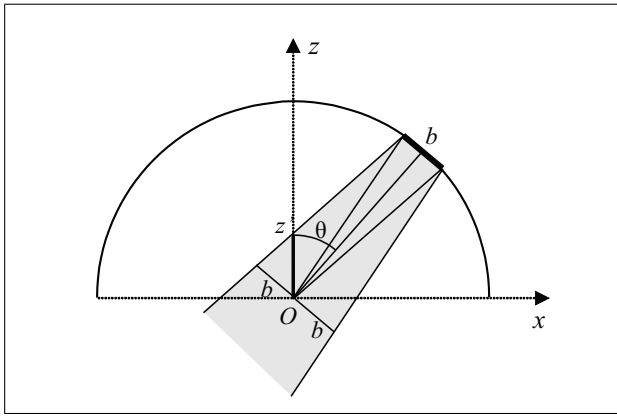


Figure 8. Section of a hemisphere. Illustration of the illuminated part of the z -axis (line Oz') by the reflection from a plane segment with width b , with the source in O .

will be $p(0)_{\text{rms}}^2 = 1/2 N \hat{p}^2 / (2R)^2$. The pressure described by (8) will be obtained with ISM if

$$N = 4R^2 k^2 = (4\pi R / \lambda)^2. \quad (14)$$

That means that the number of surfaces required will be frequency-dependent. For real situations in room acoustics, for example the frequency 500 Hz and $R = 10$ m, $N > 34000$, this is not practically feasible. The large number is due to the incorrect summation of the energy of correlated sources.

If coherent sources were used, including the phase in the summation of pressure, the number of surfaces can be reduced. Assuming a point source in the centre of the sphere, $p(r) = \hat{p}e^{-jk_r r} / r$, the contribution of each image source in the centre will be $p(0) = \hat{p}e^{-jk2R} / 2R$. When adding all image sources (with same phase) the total pressure in the centre will be $|p(0)| = N \hat{p} / 2R$. A correct prediction at the focal point (7) is obtained in case

$$N = 2kR = 4\pi R / \lambda. \quad (15)$$

Again the number of surfaces required will be frequency-dependent. For the calculation example given above $N = 370$ is needed; this is much less than with energy summation and might even be practically possible. The width of the surfaces will be $b = \sqrt{2\pi R^2 / N} = \sqrt{\lambda R} / 2$, in this example 1.3 m. This agrees with the required width of plane segments to model a cylinder as found by [14]. The illuminated width in the centre by the mirror sources will be $2b$, in this case 2.6 m. In section 3 it is mentioned that in the case of a hemisphere the actual width at the focal point is much smaller, in the order of $\lambda/2$, so when $R > 2\lambda$, which is usually the case (except for small rooms at low frequencies), the focal area calculated with mirror images is too large. So mirror imaging cannot predict both focal strength and focal width correctly at the same time.

When moving the observation point away from the centre, the observation point will be out of the visibility zone of a number of image sources. The number of visible image sources for a hemisphere will be calculated while moving the receiver along the z -axis.

The illuminated length along the z -axis by a single plane surface with dimensions $b \cdot b$ (see Figure 8) can be approximated (for small b) by $z' = b / \sin \theta$. For position z' is $\theta_v = \arcsin(b/z')$, with $z' \geq b$. On the z -axis, all mirror sources will be visible for z' for which $0 < \theta < \theta_v$. In the horizontal plane the observation point at $x = y = 0$ will be visible for all mirror images (provided that $0 < \theta < \theta_v$). For position z' the total number of mirror sources visible $n(z')$ will be the area of the hemisphere where the sources are visible, divided by the area per segment,

$$\begin{aligned} n(z') &= \frac{R^2}{b^2} \int_0^{2\pi} \int_0^{\theta_v} \sin \theta \, d\theta \, d\varphi \\ &= \frac{2\pi R^2}{b^2} \left[1 - \sqrt{1 - \frac{b^2}{z'^2}} \right]. \end{aligned} \quad (16)$$

Using this number of visible sources, the pressure at position z' can be expressed by

$$p(z')_{\text{rms}}^2 = \frac{n(z') \hat{p}^2}{8R^2} = \hat{p}^2 \frac{\pi}{4b^2} \left[1 - \sqrt{1 - \frac{b^2}{z'^2}} \right]. \quad (17)$$

For $z' \gg b$ the rms pressure can be estimated by the first two terms of the Taylor series,

$$p(z')_{\text{rms}}^2 \approx \frac{\pi \hat{p}^2}{8 z'^2}. \quad (18)$$

When z' varies from b to $z' \gg b$, the pressure $p(z')_{\text{rms}}^2$ will vary from $\pi \hat{p}^2 / 4z'^2$ to $\pi \hat{p}^2 / 8z'^2$, which comes close to the geometrical decrease with distance,

$$p(z)_{\text{rms}}^2 = \frac{1}{2} \frac{\hat{p}^2}{z^2}. \quad (19)$$

In reality the calculated pressure will vary stepwise. Figure 9 shows the calculated pressure along the z -axis of a hemisphere ($R = 10$ m) for $N = 255$ for the situation where the surfaces have equal area $b \cdot b$. For $z' > b$ (in this case $b \approx 1.5$ m) this corresponds quite well to the geometrical decrease with distance.

When using equal surfaces $b \cdot b$ the ISM model can not be closed. Figure 9 also shows the calculation result when the number of surfaces is kept constant in each row, to be able to connect the corners. Moving upward in the cupola the area of the plane surfaces is decreased. However, with ISM, the contribution to the pressure on the x -axis depends on the number of surfaces, not on the area of each surface. The total number of surfaces is 400. Quite different results can be seen, not corresponding to the geometrical decrease.

It can be concluded that even out of the focal point the ISM can produce quite erroneous results when modelling a spherical reflector.

4.2. Ray tracing (RT)

In RT, the propagating sound wave is modelled with a ray, normal to the propagating direction. The source is emitting

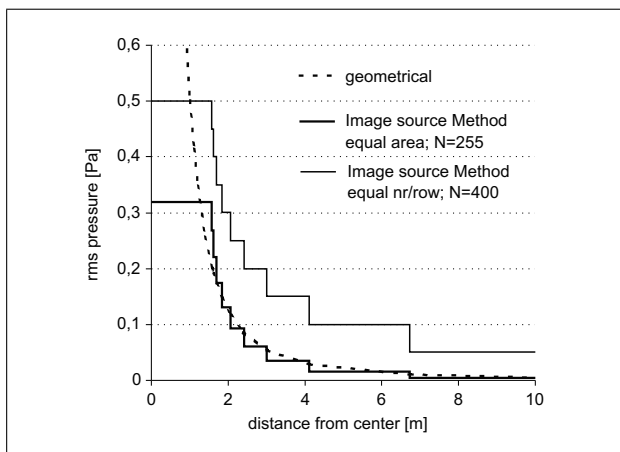


Figure 9. Rms Sound Pressure along the z-axis of a hemisphere with sound source ($\hat{p} = 1 \text{ N/m}$) in the centre, geometrical propagation (19) and ISM modelling of the hemisphere, with surfaces with equal areas and with surfaces with different areas (constant number of surfaces each row).

the rays, mostly, but not necessarily, with a uniform distribution. If we assume a monopole with sound pressure at distance r , $p(r) = \hat{p}e^{-jkr}/r$, then the sound power P of this source will be

$$P = I(r) \cdot S(r) = \frac{\hat{p}^2}{2\rho c r^2} 4\pi r^2 = \frac{2\pi}{\rho c} \hat{p}^2. \quad (20)$$

Assuming the uniform distribution of N rays emitted by the source, the power of each ray i will be

$$P_i = \frac{2\pi}{\rho c} \frac{\hat{p}^2}{N}. \quad (21)$$

The rays are detected with a receiver volume. The energy in that receiver volume depends on the travel time of the ray through the volume, $E_i = P_i \cdot \Delta t$, with $\Delta t = l_i/c$, where l_i is the path length of ray i through the receiver volume.

The average intensity (averaged over the volume of the receiver) of the sound wave of ray i inside the receiver is $I_i = E_i c/V$, where V is the volume of the receiver. This will result in

$$I_i = P_i \cdot \Delta t \cdot c/V = P_i \cdot l_i/V. \quad (22)$$

Should the model be segmented there will be a spread of energy around the focal point (width $2b$). Should this spread be limited to $\lambda/2$ width, the dimensions of the segments should not be more than $\lambda/4$. Contrary to the mirror source method, the pressure at the focal point will not increase when the number of segments further increases, since the number of rays hitting the focal area depends on the number of rays emitted from the source and the total opening angle of the concave surface.

Instead of segmenting the model it is basically possible to implement an exact model, in the sense that all rays reflect in the correct specular direction, depending on the orientation of the small surface element at the impact position of the ray (see also [17]). This model can either be a parameterised model or a sufficiently segmented model.

So the case will be considered of a receiver at the exact focal point and all reflected rays will pass this focal point. Assuming the centre of the receiver volume in this focal point, path length l will be equal to the diameter of the receiver volume.

The total pressure in the receiver volume (with diameter D) results from an energy summation and (21) and (22),

$$p_{\text{rms}}^2 = \rho c \sum_{i=1}^N I_i = 12 \frac{\hat{p}^2}{D^2}. \quad (23)$$

It is noted that this expression is independent of the number of rays (as it should be) but is dependent on the volume of the receiver. The energy is distributed equally over the receiver volume. A larger receiver volume will not be compensated by more rays (as it will be in a statistical sound field) since all rays pass at the centre. When we assume the diameter of the receiver volume $D = \lambda/2$, the total pressure in the receiver volume will be

$$p_{\text{rms}}^2 = 12 \frac{\hat{p}^2}{D^2} = 48 \frac{\hat{p}^2}{\lambda^2},$$

while the correct solution for a full sphere is $p_{\text{rms}}^2 = 2\hat{p}^2 k^2 = 8\pi^2 \hat{p}^2 / \lambda^2$.

For this case it seems possible, with the correct reflection direction of rays and the right (frequency-dependent) selection of the receiver volume, to approximate the correct solution with the RT procedure fairly well. However, when we consider a hemisphere instead of a full sphere, only half of the rays will return to the focal point. The total pressure using RT and assuming a receiver size $D = \lambda/2$ will be

$$p_{\text{rms}}^2 = \rho c \sum_{i=1}^{N/2} \frac{P_i}{\pi D^2/6} = 6 \frac{\hat{p}^2}{D^2} = 24 \frac{\hat{p}^2}{\lambda^2},$$

while the correct solution for a hemisphere will be (8)

$$p_{\text{rms}}^2 = 2\pi^2 \frac{\hat{p}^2}{\lambda^2}.$$

Now the ratio between ray solution and correct solution is different from the full sphere. This results from the energy summation. Energy summation is only correct in the case of a random phase. In this case the energy arrives at an equal phase.

It is noted that in commercially available RT programs the size of the receiver cannot be chosen.

Furthermore it is noted that only the pressure at the focal point is calculated. For this particular case (all rays passing the receiver at an exact focal point) there is no spread of energy calculated in the focal plane. Due to the energy approach the interference pattern is not calculated.

Due to the energy approach it is not possible to introduce the phase in the calculation. When incorporating the phase, BT should be applied.

4.3. Beam tracing (BT)

The main difference between RT and BT is the way the decrease in distance is handled. In RT the decrease in sound pressure of an expanding sound field with the distance from the source is implicit in the calculation method since the distance between the rays becomes larger, and in a statistical approach the probability of hitting a (fixed size) volume receiver decreases.

BT is deterministic in the sense that the entire radiating area of the source is covered. The decrease with distance is calculated from $p_{\text{rms}}^2 \simeq \Delta\Omega/S(t)$, where $\Delta\Omega$ is the opening angle of the beam and $S(r)$ is the cross-sectional area of the beam at distance r from the source. When applying this method on curved surfaces the beam will converge and due to the smaller $S(r)$ the geometrically-correct increase in sound pressure will be found. At the focal point however $S(r) = 0$ which will lead to an (incorrect) infinite sound pressure.

So this method is not capable of calculating the sound pressure at the focal point.

At sufficient distance (see section 3) from the focal point however this method can be applied and will basically give the correct geometrical value. As with RT, BT is used as an energy method. Contrary to RT, BT is deterministic in the sense that the pressure and phase can be calculated at each position. That means that a coherent calculation is possible. Results of coherent calculations on curved surfaces are reported in [18] and [19]. However this seems less meaningful when the maximum pressure in the focal point cannot be determined.

5. Reduction of reflections from concave surfaces

After having determined the expected amplitude of the concentrating reflection, the next question will be how to reduce these high sound pressure levels. Except by completely altering the design (usually the best advice), the obvious method to reduce sound concentration is to apply sound-absorptive or diffusive materials to the curved surface. Some interesting cases are presented e.g. in [3].

The effects of these treatments will be discussed in this section. As a first step the theoretical maximum reduction will be discussed, when the reflection from the curved surface is fully diffusive. Secondly the reduction by diffusing or absorbing materials will be discussed.

5.1. Diffuse reflections

In the previous sections a full reflection is assumed against a hard surface. The opposite will be the situation where reflections are completely diffuse (disregarding the practical possibilities of achieving this). In the case of perfect diffuse reflections there is random phase relation at each reception point, so energy will be added instead of pressure. With the source in the centre of a hemisphere, the

incident sound intensity on the surface element dS of the hemisphere with radius R will be

$$I_i = \frac{\hat{p}^2}{2\rho c R^2}. \quad (24)$$

So the incident power on a small surface element dS of the hemisphere will be

$$dP_i = I_i dS = \frac{\hat{p}^2 dS}{2\rho c R^2}. \quad (25)$$

All the surfaces dS will act as independent radiators. For each of these radiators a Lambert radiation directionality will be assumed. The intensity of Lambert radiation is dependent on the angle θ with the normal to the radiating surface $I_\varphi = I_0 \cos \theta$. The total power P radiated by the Lambert radiator will result from integrating over the radiating surfaces, as seen from the radiator,

$$P = I_0 d^2 \int_0^{2\pi} \int_0^{\pi/2} \sin \theta \cos \theta \, d\theta \, d\varphi = \pi d^2 I_0, \quad (26)$$

where I_0 is the on-axis sound intensity at distance d from the radiating surface. This means that the angle-dependent intensity of each Lambert radiator will be

$$I_\varphi = \frac{P}{\pi d^2} \cos \theta. \quad (27)$$

Assuming that all incident energy will be reflected, the incident power dP_i of (25) can be entered in (27) for the radiant power P , obtaining the intensity in a point at angle θ and distance d from surface element dS ,

$$dI_\varphi = \frac{\hat{p}^2 dS}{2\pi \rho c d^2 R^2} \cos \theta.$$

The total pressure at distance d results from integration over dS ,

$$p_{\text{rms}}^2 = \rho c I = \int_S \frac{\hat{p}^2 \cos \theta}{2\pi d^2 R^2} dS. \quad (28)$$

In the centre of the hemisphere this reduces to ($d = R$, $\cos \theta = 1$)

$$p_{\text{rms}}^2 = \frac{\hat{p}^2}{2\pi R^4} \int_S dS = \frac{\hat{p}^2}{R^2}. \quad (29)$$

It can easily be seen that the pressure of the specular reflecting concave reflector (5) is much higher than the pressure from the perfect diffuse reflector (29).

Solving the problem of the focussing effect could therefore theoretically be done by generating diffuse reflections.

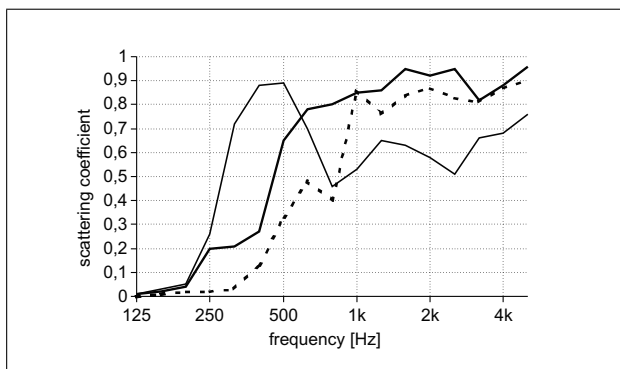


Figure 10. The scattering coefficient of three different diffusers (from [20]). Thick line: modulated array, 6 periods, 8 wells/period, 0.17 m deep. Dashed line: 6 semicylinders $r = 0.3$. Thin line: 3 semicylinders with 0.6 m flat sections.

5.2. Reduction by diffusers or absorbers

The SPL at the focal point as indicated in Figure 4 is the maximum SPL that can occur with a perfect reflecting surface. Although the expected SPL at high frequencies is higher, problems arise mostly for lower frequencies, typically around 500 Hz. For high frequencies there is generally more diffusion and the observation area is smaller.

The sound level at the focal point may be reduced by application of (additional) diffusers or absorption. Figure 10 shows some typical data of the scattering coefficient of very good diffusing structures (taken from [20]).

For practical diffusers, the reduction that can be obtained is generally not more than 90% of the energy (10 dB).

The reduction that can be obtained with practical applicable absorptive materials is also limited. In anechoic rooms efficient sound-absorbing wedges with a length of about 1 m are usually needed to obtain an absorption coefficient of 99% [21], corresponding to an SPL reduction of 20 dB.

Especially for the low frequencies, it is difficult to obtain reductions of more than 10 dB with practical absorbers.

In our previous calculation example in paragraph 3.1 (at the focal point of a hemisphere, 8 m from the source, 500 Hz), with a reduction of the reflection due to a diffuser or absorber by 10 dB, a pressure increase relative to the direct sound would still be obtained of approximately $37 - 10 = 27$ dB at 500 Hz. This will not be sufficient to take away audible echoes.

For cylindrical surfaces however the SPL in the focal line is much lower (see Figure 4) and application of absorption or diffusing elements might be sufficient to remove the echo effects.

5.3. Other ways of reducing concentrating reflections

Should the required reduction of the concentrating sound be more than 10 dB, possibilities other than diffusion or

absorption placed on the curved surface have to be considered. In spaces where a sufficient reverberation is required (e.g. for music) the possibilities of using absorption material are limited.

In [10] the (further) reduction of concentrating reflections in the Royal Albert Hall are described within the scope of the recent refurbishment. This is done by a condensed arrangement of convex reflectors (“mushrooms”) at quite some distance from the curved surface. By this, the energy that reaches the curved surface is reduced significantly and the diffuse reflections from the mushrooms have a shorter arrival time at the audience, masking the echo rather than increasing it.

Another way to overcome the limitations of the suppression of specular energy by diffusers is described in [11]. Here flat panels were rotated at about 30 degrees relative to the concave surface, redirecting the reflections away from the centre. The size of these panels had to be larger than about two wavelengths to be sufficiently effective in suppressing the echo.

6. Conclusions

This paper has described an engineering method for obtaining the reflected sound field from concave spherical surfaces.

The sound pressure in the focal point of a sphere segment is dependent on the frequency and the opening angle of the segment. The pressure is not dependent on the radius of the (hemi)sphere.

As a reference the pressure at the focal point of the cylinder is given; this pressure is dependent on the radius of the cylinder. The pressure at the focal point from a sphere is much higher than from a cylinder. For a hemisphere the energy is distributed mainly over a circular area with a width of $\lambda/2$.

Outside the focus point a strong interfering sound field can be found. Within reasonable accuracy, the average sound pressure can be estimated with the geometrical method. However this geometrical method fails at the focal point.

When using the image source method to approximate the correct value at the focal point, using a small, frequency-dependent size of the segments $b = \sqrt{\lambda R/2}$ is required. It is not possible to calculate both the pressure at the focal point and the width of the focussing area correctly, and the geometrical sound field may depend on the way the geometry is entered.

Using Ray Tracing, the pressure at the focal area can be approximated to some extent when using large number of segments (or exactly modelling the curved surface) in combination with a small, frequency-dependent receiver volume $D = \lambda/2$.

Beam Tracing, especially coherent BT, may be applicable outside the focal area. Since it is a full geometrical method, an infinite SPL will be calculated at the focal point.

The focussing effect is quite strong for a small wavelength. Generally the possible reduction of the focussing effect by absorbers or diffusers is insufficient to eliminate the focussing effect. For cylindrical shapes, which have much lower pressure in the focal line, these measures might be sufficient. In the case diffusers are not sufficient to reduce the focussing effect sufficiently, more drastic interventions are necessary such as changing the basic geometry or adding large reflectors or redirecting panels.

References

- [1] M. Vercammen: Sound reflections from concave spherical surfaces. Part I: Wave field approximation. *Acta Acustica united with Acustica* **96** (2010) 82–91
- [2] H. Bagenal, A. Wood: *Planning for good acoustics*. Methuen and Co., London, 1931.
- [3] L. Cremer, H. Müller: *Die wissenschaftlichen Grundlagen der Raumakustik*. Hirzel Verlag, Stuttgart, 1978.
- [4] H. Kuttruff: *Room acoustics*. Taylor and Francis, 2000.
- [5] L. Makrinenko: *Acoustics of auditoriums in public buildings*. Acoustical Soc. of America, 1994.
- [6] A. Kircher: *Musurgia Universalis*. 1650.
- [7] G. Biancani Giuseppe: *Sphaera mundi, seu cosmographia demonstrativa*. III. Echometria, idest Geometrica tractatio de Echo, 1620.
- [8] P. Patte: *Eassai sur l'architecture theatrale*. (reprint Minkoff 1974), 1782.
- [9] T. Wulfrank, R. J. Orłowski: Acoustic analysis of Wigmore Hall, London, in the context of the 2004 refurbishment. *Proc. Inst. of Acoustics* **28** (2006).
- [10] R. A. Metkemeijer: The acoustics of the auditorium of the Royal Albert Hall before and after redevelopment. *Proceedings of the Institute of Acoustics* (2002).
- [11] K.-H. Lorenz, M. Vercammen: From 'knocking ghost' to excellent acoustics – the new Tonhalle Düsseldorf: Innovative design of a concert hall refurbishment. *Institute of Acoustics* (2006).
- [12] H.-P. Tennhardt et al.: *Der Kuppelsaal – eine Aufgabe für die raumakustische Modellmesstechnik*. DAGA - Fortschritte der Akustik, München, 2005.
- [13] J. H. Rindel: Attenuation of sound reflections from curved surfaces. *Proceedings of 24th Conf. on Acoustics, Strbské Pleso*, 1985, 194–197.
- [14] H. Kuttruff: Some remarks on the simulation of sound reflection from curved walls. *Acustica* **77** (1993) 176.
- [15] Y. Yamada, T. Hidaka: Reflection of a spherical wave by acoustically hard, concave cylindrical walls based on the tangential plane approximation. *J. Acoust. Soc. Am.* **118** (2005).
- [16] T. Yokota, S. Sakamoto, H. Tachibana, M. Ikeda, K. Takahashi, T. Ooturu: Comparison of room impulse response calculated by the simulation methods based on geometrical acoustics and wave acoustics. *Proc. ICA 2004*, 2004.
- [17] Mommertz, Müller: *Simulation der Schallübertragung in Räumen mit gekrümmten Wandflächen*. Daga, 1995.
- [18] Mommertz: *Untersuchung akustischer Wandeigenschaften und Modellierung der Schallrückwürfe in der binauralen Raumsimulation*. Doctoral thesis, RWTH Aachen University, 1996.
- [19] P. Jean, N. Noe, F. Gaudaire: Calculation of tyre noise radiation with a mixed approach. *Acta Acustica united with Acustica* **93** (2007) 1–13.
- [20] T. J. Cox, P. D'Antonio: *Acoustic absorbers and diffusers, theory, design and application*. Spon Press, 2004.
- [21] ISO 3745:2003: *Acoustics – Determination of sound power levels of noise sources using sound pressure – Precision methods for anechoic and hemi-anechoic rooms*.